Published in final edited form as:

ACS Chem Biol. 2015 April 17; 10(4): 1118–1127. doi:10.1021/cb500820b.

Structure-guided design of a high affinity inhibitor to human CtBP

Brendan J. Hilbert[†], **Benjamin L. Morris**[‡], **Keith C. Ellis**[§], **Janet L. Paulsen**[†], **Celia A. Schiffer**[†], **Steven R. Grossman**[‡,*], and **William E. Royer Jr.**[†,*]

[†] Department of Biochemistry and Molecular Pharmacology, University of Massachusetts Medical School, Worcester, Massachusetts 01605, USA

[‡]Division of Hematology, Oncology, and Palliative Care, Department of Human and Molecular Genetics, and Massey Cancer Center, Virginia Commonwealth University, Richmond, VA 23298, USA

[§]Department of Medicinal Chemistry, Virginia Commonwealth University, Richmond, VA 23298, USA

Abstract

Oncogenic transcriptional coregulators C-terminal Binding Protein (CtBP) 1 and 2 possess regulatory D-isomer specific 2-hydroxyacid dehydrogenase (D2-HDH) domains that provide an attractive target for small molecule intervention. Findings that the CtBP substrate 4-methylthio 2-oxobutyric acid (MTOB) can interfere with CtBP oncogenic activity in cell culture and in mice confirm that such inhibitors could have therapeutic benefit. Recent crystal structures of CtBP 1 and 2 revealed that MTOB binds in an active site containing a dominant tryptophan and a hydrophilic cavity, neither of which are present in other D2-HDH family members. Here we demonstrate the effectiveness of exploiting these active site features for design of high affinity inhibitors. Crystal structures of two such compounds, phenylpyruvate (PPy) and 2-hydroxyimino-3-phenylpropanoic acid (HIPP), show binding with favorable ring stacking against the CtBP active site tryptophan and alternate modes of stabilizing the carboxylic acid moiety. Moreover, ITC experiments show that HIPP binds to CtBP with an affinity greater than 1000-fold over that of MTOB and enzymatic assays confirm that HIPP substantially inhibits CtBP catalysis. These results, thus, provide an important step, and additional insights, for the development of highly selective antineoplastic CtBP inhibitors.

[*]Corresponding Authors: srgrossman@vcu.edu, william.royer@umassmed.edu.

ASSOCIATED CONTENT

Supporting Information

Supporting information includes two tables, six figures, a description of kinetic simulations and additional methods. This material is available free of charge *via* the internet.

Accession Codes

The atomic coordinates have been deposited in the Protein Data Bank with accession codes 4U6S (CtBP1/NAD^+/PPy) and 4U6Q (CtBP1/NADH/HIPP).

Introduction

C-terminal Binding Proteins (CtBP) 1 and 2 are critical modulators of numerous cellular processes; overexpression of these paralogous transcription coregulators has been linked to multiple human cancers.[1–5] CtBP1 was first identified through its interaction with the C-terminal region of the adenovirus E1A oncoprotein and ability to modulate E1A transforming activities.[6, 7] CtBP functions as a transcriptional regulator by tethering chromatin remodeling proteins, such as histone deacetylases, methyl transferases, and demethylases, to DNA bound transcription factors.[8, 9] Alternative splice forms of CtBP 1 and 2 also have non-nuclear roles, including membrane trafficking.[10] CtBP 1 and 2 are unique among transcription factors in the incorporation of a D-isomer specific 2-hydroxyacid dehydrogenase (D2-HDH) domain, which reduces or oxidizes substrates utilizing coenzyme $NAD(P)^+$/NAD(P)H.[11] D2-HDH family members are not otherwise involved in transcriptional regulation.

Substantial evidence implicates CtBP transcriptional function in cancer. CtBP represses expression of tumor suppressive pro-apoptotic factors (Bik, Noxa), cytoskeletal/cell adhesion molecules (keratin-8, E-cadherin)[12], and cell cycle inhibitors, ($p16^{INK4a}$, $p15^{INK4b}$)[9], while activating expression of growth and metastasis-related genes (TIAM1, MDR1, certain Wnt target genes)[13–15] facilitating the epithelial to mesenchymal transition (EMT). Thus, CtBP's transcriptional effects confer resistance to apoptosis and promote metastasis and oncogenesis.[16] CtBP is targeted for degradation by multiple tumor suppressors including APC[17, 18], HIPK2[19], JNK1[20], and ARF.[21] Consistent with these cellular effects of CtBP, overexpression of CtBP is observed in the majority of human breast, colon, ovarian, and prostate cancers.[1–5]

4-Methylthio 2-oxobutyric acid (MTOB), a substrate for CtBP catalysis, antagonizes CtBP transcriptional regulation.[3, 422] MTOB induced apoptosis through displacement of CtBP2 from the *Bik* promoter in HCT116 colon cancer cells.[4] In mouse xenograft models, administration of MTOB resulted in decreased tumor burden and prolonged survival compared with untreated mice.[4] Additionally, MTOB evicted CtBP from target promoters in breast cancer cell lines, shifting expression patterns for key genes from mesenchymal to a more epithelial phenotype.[3] Although high concentrations (>300 μM) are required for (substrate) inhibition of CtBP, the clear inhibitory effect of MTOB on cancer cells demonstrates that small molecules could be developed to effectively treat cancers specifically regulated by CtBP activity.

Crystal structures of CtBP 1 and 2 in complex with MTOB have revealed details of active site features that are very similar in both paralogs and provide a basis for the design of higher affinity compounds.[23] The finding that MTOB does not lead to large conformational changes suggested that transcriptional inhibition of CtBP by MTOB might result from either enhanced substrate turnover or interfering with transcriptional activities that require cycling between dimeric and monomeric CtBP.[23] The structures revealed two particularly attractive properties, a dominant tryptophan (318 in CtBP1) and a hydrophilic channel filled by four ordered water molecules, that are not shared by other members of the D2-HDH protein family, and thus offer a potential basis for the development of highly specific inhibitors.[23]

Here we present structural and thermodynamic data on two compounds that exploit these active site features. Both compounds bind with favorable ring stacking to W318 and with significantly higher affinity than MTOB, including one compound that binds more than 1000 times more tightly. These findings provide a solid foundation for the development of highly potent and pharmacologically useful CtBP inhibitors that could be of great therapeutic benefit across a broad spectrum of human neoplastic disease.

RESULTS AND DISCUSSION

Identification and co-crystal structures of potential CtBP1 ligands

Based on our earlier crystal structures of MTOB bound to CtBP1 and CtBP2,[23] we explored small molecules that could exploit the extensive surface area formed by a unique active site tryptophan (318/324 in CtBP1/2). Qualitative assessment of potential compounds using the Schrodinger Suite Glide program[24] suggested that incorporation of a phenyl ring to pack against W318, such as in the established substrate phenylpyruvate (PPy),[22] would enhance binding affinity. Additionally we identified a related molecule that would avoid catalytic turnover. In 2-hydroxyimino-3-phenylpropionic acid (HIPP), the PPy carbonyl, target of CtBP dehydrogenase function, is substituted with an oxime. To observe the specific contacts and effects of ligands on the active site, we determined PPy and HIPP co-crystal structures with CtBP1 at 2.1Å and 2.3Å, respectively (see Supplementary Table 1 for crystallographic statistics).

The crystal structures of PPy and HIPP bound to CtBP1 demonstrate that, similarly to MTOB, ligand binding does not induce large changes in domain conformation (Figure 1). Superposition with the MTOB CtBP1 structure reveals root-mean-square (rms) deviations of 0.35 Å and 0.32 Å for the PPy and HIPP structures, respectively. Superposition of dimeric PPy and HIPP complexes with the MTOB structure, generated by crystallographic symmetry, reveal only slightly larger rms deviations of 0.39 Å and 0.36 Å respectively. Only the hinge region between the substrate binding domain and coenzyme binding domain in the PPy structure deviates from the typical hinge conformation observed across other CtBP structures. In the PPy structure the hinge exists in two distinct conformations due to a shift in A123 position (Figure 1C–D) whose impact on the CtBP active site is discussed below.

Ligand Conformations and Contacts

As intended, PPy and HIPP bind in the active site of CtBP1 with their respective phenyl groups stacking against the W318 side chain. However, the structures reveal an unexpected conformation of the alpha-keto acid moieties that is accessible for binding in both molecules. In the crystal structure of the complex CtBP1/NAD^+/PPy, PPy assumes two distinct conformations which are present in roughly equal proportions, occupying a total of 80% of CtBP1 active sites within the crystal. In one conformation, similar to that of MTOB, the PPy carbonyl is anchored in place adjacent to catalytic residues H315 and R266 in preparation for catalysis (Figure 2B). A second, unanticipated, conformation, clearly evident in the electron density maps (Supplementary Figure 1), orients both PPy carboxylate oxygen atoms towards the catalytic residue R266 (Figure 2C). In this non-canonical conformation, the PPy carbonyl is no longer positioned for hydride transfer.

Although similar in packing their phenyl groups with W318, substrate and non-canonical conformations of PPy display markedly distinct keto acid core contacts with CtBP1. The substrate conformation forms a hydrogen bond network resembling that observed in the MTOB structure, with slight variation in the bonding scheme (Figure 3B). This includes similar hydrogen bonds involving the carboxylate with active site loop residues S100 and G101 and the carbonyl with catalytic residues R266 and H315. In addition to the hydrogen bond network, R266 and R97 contribute to binding through coulombic interactions deriving from the proximity of the ligand carboxylate and arginine guanidinium groups. The hydrogen bond network is reorganized in the non-canonical conformation (Figure 3C), with the PPy carboxylate now forming hydrogen bonds with the catalytic residues and the active site loop, while the carbonyl forms a hydrogen bond with only S100. The carboxylate forms ionically stabilized hydrogen bonds involving both carboxylate oxygens with R266, and appears to be in a favorable coulombic interaction with R97. The roughly equal occupancies of the two PPy conformations suggest that the binding affinities of the two conformations in the active site of CtBP1 do not differ substantially.

In the crystal structure of the complex CtBP1/NADH/HIPP, HIPP assumes only the non-canonical conformation and, unlike PPy and MTOB, fully occupies the active site (Figure 2D). The substrate conformation is characterized by the carbonyl groups of MTOB and PPy in position to form a hydrogen bond with catalytic residue H315. The larger oxime group at this position in HIPP would require a shift in side chains or ligand orientation to prevent a clash with H315 if HIPP were to adopt a substrate conformation. No such shift in active site residues occurs in the HIPP co-crystal structure, and thus HIPP exhibits the non-canonical conformation (Supplementary Figure 2).

HIPP possesses a similar network of contacts with CtBP1 as does the noncanonical PPy conformation, including maximal interactions between the phenyl ring and W318. A slight difference in position relative to the non-canonical PPy conformation results in small changes in the HIPP hydrogen bond network, reflected in the absence of a hydrogen bond between the carboxylate and NADH ribose. The shift in carboxylate that prevents formation of this hydrogen bond positions the carboxylate 0.8Å closer to the R97 guanidinium group. The distances between the HIPP carboxylate oxygen atoms and the R266 guanidinium are roughly equivalent. Overall, this suggests an increase in HIPP coulombic interaction with CtBP1 relative to the non-canonical PPy conformation. Finally, the HIPP oxime is stabilized through a hydrogen bond with an active site water molecule, the impact of which will be discussed below.

Analysis of the van der Waals contacts confirms substantially greater interaction of the PPy and HIPP phenyl groups with W318 compared to the W318 interaction of the MTOB thioether sulfur, consistent with the original rationale for exploring these compounds. The phenyl packing is calculated to contribute 2–3 fold greater favorable interactions with W318 than does MTOB, and dominates the van der Waals contribution to binding energy (Figure 4). The substrate PPy conformation, non-canonical PPy conformation, and HIPP all have similar van der Waals contact profiles measured by per residue interactions, despite differences in conformation, again suggesting little difference in energy between the substrate and non-canonical PPy conformations (Figure 4). Thus the optimal packing and pi

stacking between W318 and ligand phenyl rings of PPy and HIPP provides a major contribution to ligand binding.

Impact of binding on water network and hinge conformation

CtBP possesses a hydrophilic cavity that is continuous with the enzyme's catalytic site and adjacent to a domain hinge. A water network threads through the cavity, providing hydrogen bond linkage between MTOB and an NAD(H) phosphate.[23] The cavity is absent in other members of the D2-HDH family, due to larger side chains that fill the volume and stabilize bound substrate.[23, 25] This cavity, therefore, provides a unique structural feature that could be exploited for future inhibitor design to increase affinity and specificity for CtBP over other D2-HDH family members. Although binding of inhibitors that fill this cavity must balance favorable direct interactions with any possible energetic penalties resulting from displacement of bound waters, it appears that any unfavorable energetics of water displacement are minor, or even favorable due to solvent entropic gains, based on the high affinity of HIPP for CtBP (see below).

The MTOB bound structure consists of four waters (W1–W4) in the cavity, with W1 interacting with MTOB and W4 contacting the NAD^+ phosphate (Figure 5A). W1 is displaced by the HIPP oxime and the non-canonical PPy carbonyl. The substrate conformation of PPy, however, retains W1 analogous to the MTOB-bound CtBP1 structure (Figure 5B and Supplementary Figure 3).

HIPP further alters the water network through direct interaction with W2 (Supplementary Figure 3), shifting it relative to that in the MTOB structure (Supplementary Figure 4C). This HIPP W2 position clashes with the W3 position (1.9Å apart), but electron density maps show that each of these mutually exclusive water sites is partially occupied (Supplementary Figure 5). HIPP therefore displaces two waters from the active site, while altering the position of a third water relative to the MTOB structure. Only W4, closest to NADH, remains unperturbed by HIPP binding.

The effects on the water network are more dramatic in the non-canonical PPy structure as a direct result of conformational changes in hinge residues. Movement of residue A123 results in two conformations of the hinge region in the PPy structure, with the novel conformation of A123 exhibiting roughly 70% occupancy (Supplementary Figure 6). This new conformation partially collapses the cavity that contains the water network, displacing W2 and W3 from the structure (Figure 5B). It is uncertain whether W2 and W3 occupy their expected positions when A123 assumes its canonical conformation the other 30% of the time. Although the proportion of the non-canonical conformation of A123 is roughly equivalent to the total occupancy of PPy in the active site (both conformations), it remains unclear what causes the shift in hinge conformation. van der Waals analysis indicates only a minor increase in PPy contacts when A123 assumes the novel conformation, which would likely not explain the movement. Two of eight monomers in the CtBP2-MTOB complex[23] demonstrate flexibility at the equivalent residue (A129) where we observed flipping of the backbone carbonyl position. The HIPP structure does not contain the novel hinge conformation suggesting new inhibitors designed to fill the hydrophilic cavity will induce adoption of the canonical hinge conformation.

Inhibitor Affinity

In order to investigate the validity of our inhibitor design strategy, we employed isothermal titration calorimetry (ITC) to measure the thermodynamics for binding of HIPP and MTOB to both CtBP1 and CtBP2. Our CtBP2 dehydrogenase construct proved more amenable to ITC than CtBP1 largely due to higher solubility and stability, particularly at pH 8.5. Initial experiments measured the dissociation constant (Kd) of HIPP alone and in the presence of 1.5 mM NAD^+ as 1.30 μM (Figure 6A) and 1.44 μM, respectively, showing little effect from the presence of coenzyme (Table 1). Attempts to directly measure MTOB affinity for CtBP2 were met with low signal (Supplementary Figure 7), but suggest an MTOB binding dissociation constant in the low millimolar range. Utilizing HIPP's high affinity, we performed competitive displacement ITC experiments[26] with MTOB to more accurately estimate binding affinity. From these experiments MTOB Kd was calculated to be 2.96 mM, three orders of magnitude weaker than HIPP (Table 1). Substantial precipitation of CtBP2 upon addition of PPy interfered with our ability to quantitatively measure PPy binding by ITC. However, we were able to easily visualize injection peaks in the isotherm at low PPy concentrations (Supplementary Figure 7), demonstrating that PPy binding is tighter than MTOB. Although PPy affinity appears higher than MTOB, increased substrate inhibition or the non-catalytically competent conformation, may explain the lower efficiency of PPy turnover by CtBP.[22]

Although CtBP1 was less stable than CtBP2 during ITC experiments, we were able to confirm HIPP and MTOB binding are similar across the CtBP family. HIPP binding at pH 8.5 yielded a dissociation constant of 2.77 μM, similar to the values observed with CtBP2 (Figure 6B). CtBP1 proved too unstable to perform other experiments at pH 8.5, but lowering the pH to 7.5 improved CtBP1 stability moderately and significantly increased HIPP affinity (Figure 6C). The HIPP Kd decreased nearly an order of magnitude to 0.37 μM when measured at pH 7.5 (Table 1). Utilizing the displacement ITC approach, the Kd of MTOB binding to CtBP1 was calculated to be 1.26 mM at pH 7.5, a more than two-fold increase in affinity relative to CtBP2 at pH 8.5. Although the free energy of binding is more favorable at pH 7.5, the entropic contributions to HIPP/CtBP1 binding become more unfavorable (Table 1). Likewise, unfavorable entropy increases when MTOB binding is measured at pH 7.5 despite a more favorable NG, suggesting pH is at least partially responsible for the increase in MTOB affinity observed in CtBP1 relative to CtBP2. However, inherent differences between CtBP1 and CtBP2 binding may also contribute to the different measured MTOB affinities.

The strong pH sensitivity suggests involvement of a group whose strength of interaction increases due to protonation. The most likely candidate is H315, whose proximity to E295 will raise its pKa and ensure that it will be doubly protonated for catalysis under physiological conditions.[27] Increased protonation of H315 would stabilize its interaction with the HIPP carboxylate (2.9Å between H315 Nε2 and HIPP) or hydrogen bond donation to the MTOB carbonyl (2.6Å between H315 Nε2 and MTOB). Thus, measurements at pH 8.5 appear to underestimate ligand affinity to CtBP2 under physiological conditions due to reduced protonation of H315.

The thermodynamics of MTOB and HIPP binding suggest direct contacts with CtBP drive substrate and inhibitor binding, since both are enthalpically driven and entropically unfavorable (Table 1). The increase in HIPP van der Waals interactions (Figure 4), dominated by contact with W318, would likely explain a portion of the enthalpic gains over MTOB; however the distinct hydrogen bond network and coulombic interactions of the non-canonical conformation make it difficult to interpret other sources contributing to the gain in affinity for PPy and HIPP. With the current understanding of HIPP binding, we will monitor the affinity and thermodynamics of next generation inhibitors to optimize specific, designed interactions, illuminating the major enthalpic contributors to HIPP binding.

The energetics of water displacement and hinge movement do not appear to hinder future inhibitors which will be designed to bind in the water network pocket. Any possible energetic penalty associated with water network changes, including the release of W1 and rearrangement of W2 and W3 positions, appears to be dwarfed by new inhibitor-protein interactions as evidenced by the dramatic increase in HIPP affinity. Furthermore, the canonical conformation of the hinge region in the HIPP structure suggests that hinge movement observed with PPy will not greatly impact future inhibitor binding. The energy necessary to prevent hinge conformational changes may therefore be minimal, since it is easily overcome by the influence of HIPP and water interactions in the active site. This suggests that future inhibitors can be designed to occupy the water network cavity without large energy penalties.

Enzymatic inhibition

Kinetic inhibition assays were performed to assess the ability of HIPP to inhibit CtBP catalytic activity, as detailed in Supporting Information. Inhibition assays directly measured CtBP dependent NADH oxidation in the presence of the substrate, MTOB, and inhibitor. Consistent with our crystallographic and ITC results, both PPy and HIPP substantially inhibit CtBP dehydrogenase function, exhibiting IC_{50} values of 135 μM and 745 nM, respectively (Figure 7A and B). Further analysis of Ki was not possible with PPy, as it demonstrated substrate turnover at low concentrations, but was pursued with HIPP. Given that HIPP binds in the same substrate pocket as MTOB, a purely competitive inhibition model could have been expected in which K_m would increase, but V_{max} would remain largely unaffected. However, plots of HIPP inhibition (Figure 7C) indicate that the major kinetic effect involves V_{max}, which is confirmed by fitting the data to a noncompetitive mechanism (Ki of 928nM, R^2= 0.7556) in contrast to competitive inhibition (Ki=109.1nM; R^2=0.4995).

A plausible explanation for our kinetic results can be found by considering likely conformational changes required for CtBP to bind and release both substrate and cofactor during a complete reaction cycle. Binding of NAD(H) confers a conformational change in CtBP, most likely involving domain closure.[27] Such a domain closure is likely to hinder the release of NAD^+ following product release, permitting the binding of inhibitor or substrate to form an abortive ternary complex; such ternary complexes have been reported for another D2-HDH family member.[28] Modulation of domain rearrangements appears to provide the mechanism for allosteric regulation in yet another D2-HDH family member, D3-

phosphoglycerate dehydrogenase, in which binding of L-serine to a separate regulatory domain alters V_{max}.[29–31] Kinetic simulations (Supporting Information) suggest that formation of such abortive ternary complexes in CtBP could explain both the largely non-competitive inhibition by HIPP and substrate inhibition by MTOB (Figure 7D). Although complete investigation of such a model is outside the scope of this paper, these results do suggest that the inhibitory effects of MTOB on cancer cells could result from the formation of abortive ternary complexes that effectively lower the concentration of enzymatically active CtBP.

Concluding Remarks

Strong evidence for a role of the transcriptional co-regulator CtBP in human cancer suggests that it could be a useful target for therapeutic intervention.[1–5] Recent reports have identified two compounds through screening efforts that inhibit CtBP in the micromolar range, including a small molecule from the LOPAC library[32] and a cyclic peptide[33]. In this report, we have successfully applied structure-based principles to identify the highest affinity CtBP inhibitor available to date. CtBP contains a unique active site tryptophan whose aromatic packing with the phenyl groups in both PPy and HIPP appears to contribute substantially to binding affinity. HIPP, the strongest inhibitor, projects its hydroxyimino hydroxyl into a hydrophilic channel that is also unique among D2-HDH enzymes. The dramatic increase in affinity observed with HIPP demonstrates that this binding arrangement is favorable and, moreover, that the hydrophilic cavity is accessible to an inhibitor without substantial penalty for displacing ordered water molecules. This finding, thus, suggests that incorporating additional groups that extend into this cavity may provide an especially favorable approach in the design of potent and specific inhibitors for CtBP.

Exploiting the unique active site hydrophilic channel may facilitate creation of future inhibitors that could target coenzyme-mediated oligomerization, inhibiting CtBP transcriptional regulation. CtBP recruitment of coenzyme NAD^+ or NADH induces dimerization,[34] linking enzymatic function and transcriptional activity.[35] With a reported 100 fold higher affinity for NADH than NAD^+,[36] CtBP may be able to respond to the redox state of the cell, increasing transcriptional activity when stimuli, such as hypoxia and high extracellular glucose levels, increase the NADH/NAD^+ ratio.[37, 38] Although the therapeutic benefit for inhibition of CtBP dehydrogenase activity by itself is not clear, inhibitors such as HIPP can be used as scaffolds for adding chemical moieties which interfere with NAD(H) binding. Disruption of coenzyme binding could be designed to occur at the nicotinamide ring position, directly adjacent to the alpha keto acid moiety, or at the coenzyme phosphates, situated at the far edge of the hydrophilic cavity. By targeting coenzyme binding, future inhibitors should block dimerization in addition to catalytic activity, which may provide a powerful approach to inhibiting transcriptional co-regulatory activity.

METHODS

Crystallization, Structure determination and analysis

CtBP1 and CtBP2 were expressed and purified as described in Supporting Information. CtBP1-PPy was crystallized by hanging drop vapor diffusion against a reservoir solution

containing 200 mM $CaCl_2$, 100 mM Hepes pH 7.5, and 2.5 mM NAD^+. CtBP-HIPP was crystallized by vapor diffusion against a reservoir solution contining 75 mM $CaCl_2$, 100 mM Hepes pH 7.5, and 1 mM NADH. Further details of the crystallization and data collection are available in Supporting Information. Model building and refinement were performed with Coot[39] and Phenix.[40] Difference distance plot matrices and hydrogen bonds were analyzed as described previously.[23]

CtBP 2 ITC

ITC experiments were performed at 20°C with the Microcal iTC200 System (GE). Purified CtBP2 was dialyzed overnight against 500 mL of 50 mM Glycylglycine pH 8.5, 300 mM NaCl, 1 mM EDTA, 2 mM TCEP, with or without 1.5 mM NAD^+. Concentrated ligands were diluted to working concentrations in dialysate. Binding was measured by titrating in 1.5 mM HIPP. 5 mM MTOB was utilized for competitive displacement assays. MTOB was incubated with the protein sample and HIPP for 10 minutes prior to the displacement assays. 1.5 mM HIPP was titrated to displace MTOB from the CtBP2 active site. CtBP2 concentration was 100–120 μM for all experiments. Each measurement consisted of 20–25 1.0 μL injections of HIPP into the CtBP2 solutions. Data were fit in Origin software to the single binding site model. Heats of ligand dilution were measured and subtracted for each type of binding experiment before curve fitting. Final results represent the average of at least three measurements. The MTOB Kd and ΔH values were calculated from displacement assays utilizing Sigurskjold's displacement model.[26]

CtBP1 ITC

Purified CtBP1 was dialyzed against 500 mL of 50 mM Glycylglycine pH 8.5, 300 mM NaCl, 1 mM EDTA, 2 mM TCEP or 500 mL of 50 mM Hepes pH 7.5, 300 mM NaCl, 1 mM EDTA, 2 mM TCEP overnight. Final CtBP1 concentration used in ITC measurements was 50 μM. As in CtBP2 measurements ligands were diluted in dialysate. HIPP concentration for titrations was 1.4 mM at pH 8.5 and 0.5 mM at pH 7.5. 2.5 mM MTOB was incubated with HIPP and CtBP1 as above for displacement measurements. For HIPP binding at pH 8.5, 22–24 1.0 μL injections were performed per measurement. For HIPP binding at pH 7.5, 25–27 1.6 μL injections were performed per measurement. For HIPP displacement of MTOB, 25–27 1.1 or 1.2 μL injections were performed. As above, heats of dilution were subtracted before curve fitting in Origin. Final results represent the average of 2–4 measurements.

Supplementary Material

Refer to Web version on PubMed Central for supplementary material.

Acknowledgments

We thank A. Carruthers, R. Moran and N. Kurt Yilmaz for useful discussions. The diffraction data were collected on a Rigaku CCD system obtained through NIH shared instrumentation grant S10 OD012028 (CS, PI). SG was supported by a Research Scholar Grant from the American Cancer Society.

REFERENCES

1. Barroilhet L, Yang J, Hasselblatt K, Paranal RM, Ng SK, Rauh-Hain JA, Welch WR, Bradner JE, Berkowitz RS, Ng SW. C-terminal binding protein-2 regulates response of epithelial ovarian cancer cells to histone deacetylase inhibitors. Oncogene. 2013; 32:3896–3903. [PubMed: 22945647]
2. Birts CN, Harding R, Soosaipillai G, Halder T, Azim-Araghi A, Darley M, Cutress RI, Bateman AC, Blaydes JP. Expression of CtBP family protein isoforms in breast cancer and their role in chemoresistance. Biol Cell. 2010; 103:1–19. [PubMed: 20964627]
3. Di LJ, Byun JS, Wong MM, Wakano C, Taylor T, Bilke S, Baek S, Hunter K, Yang H, Lee M, Zvosec C, Khramtsova G, Cheng F, Perou CM, Ryan Miller C, Raab R, Olopade OI, Gardner K. Genome-wide profiles of CtBP link metabolism with genome stability and epithelial reprogramming in breast cancer. Nat Commun. 2013; 4:1449. [PubMed: 23385593]
4. Straza MW, Paliwal S, Kovi RC, Rajeshkumar B, Trenh P, Parker D, Whalen GF, Lyle S, Schiffer CA, Grossman SR. Therapeutic targeting of C-terminal binding protein in human cancer. Cell Cycle. 2010; 9:3740–3750. [PubMed: 20930544]
5. Wang R, Asangani IA, Chakravarthi BV, Ateeq B, Lonigro RJ, Cao Q, Mani RS, Camacho DF, McGregor N, Schumann TE, Jing X, Menawat R, Tomlins SA, Zheng H, Otte AP, Mehra R, Siddiqui J, Dhanasekaran SM, Nyati MK, Pienta KJ, Palanisamy N, Kunju LP, Rubin MA, Chinnaiyan AM, Varambally S. Role of transcriptional corepressor CtBP1 in prostate cancer progression. Neoplasia. 2012; 14:905–914. [PubMed: 23097625]
6. Boyd JM, Subramanian T, Schaeper U, La Regina M, Bayley S, Chinnadurai G. A region in the C-terminus of adenovirus 2/5 E1a protein is required for association with a cellular phosphoprotein and important for the negative modulation of T24-ras mediated transformation, tumorigenesis and metastasis. EMBO J. 1993; 12:469–478. [PubMed: 8440238]
7. Schaeper UBJ, Uhlmann E, Subramanian T, Chinnadurai G. Molecular cloning and characterization of a cellular phosphoprotein that interacts with a conserved C-terminal domain of adenovirus E1A involved in negative modulation of oncogenic transformation. PNAS. 1995; 92:10467–10471. [PubMed: 7479821]
8. Kuppuswamy M, Vijayalingam S, Zhao LJ, Zhou Y, Subramanian T, Ryerse J, Chinnadurai G. Role of the PLDLS-binding cleft region of CtBP1 in recruitment of core and auxiliary components of the corepressor complex. Mol Cell Biol. 2008; 28:269–281. [PubMed: 17967884]
9. Chinnadurai G. The transcriptional corepressor CtBP: a foe of multiple tumor suppressors. Cancer Res. 2009; 69:731–734. [PubMed: 19155295]
10. Corda D, Colanzi A, Luini A. The multiple activities of CtBP/BARS proteins: the Golgi view. Trends Cell Biol. 2006; 16:167–173. [PubMed: 16483777]
11. Chinnadurai G. CtBP, an unconventional transcriptional corepressor in development and oncogenesis. Mol Cell. 2002; 9:213–224. [PubMed: 11864595]
12. Grooteclaes M, Deveraux Q, Hildebrand J, Zhang Q, Goodman RH, Frisch SM. C-terminal-binding protein corepresses epithelial and proapoptotic gene expression programs. Proc Natl Acad Sci U S A. 2003; 100:4568–4573. [PubMed: 12676992]
13. Fang M, Li J, Blauwkamp T, Bhambhani C, Campbell N, Cadigan KM. C-terminal-binding protein directly activates and represses Wnt transcriptional targets in Drosophila. EMBO J. 2006; 25:2735–2745. [PubMed: 16710294]
14. Jin W, Scotto KW, Hait WN, Yang JM. Involvement of CtBP1 in the transcriptional activation of the MDR1 gene in human multidrug resistant cancer cells. Biochem Pharmacol. 2007; 74:851–859. [PubMed: 17662696]
15. Paliwal S, Ho N, Parker D, Grossman SR. CtBP2 Promotes Human Cancer Cell Migration by Transcriptional Activation of Tiam1. Genes Cancer. 2012; 3:481–490. [PubMed: 23264848]
16. Hanahan D, Weinberg RA. Hallmarks of cancer: the next generation. Cell. 2011; 144:646–674. [PubMed: 21376230]
17. Nadauld LD, Phelps R, Moore BC, Eisinger A, Sandoval IT, Chidester S, Peterson PW, Manos EJ, Sklow B, Burt RW, Jones DA. Adenomatous polyposis coli control of C-terminal binding protein-1 stability regulates expression of intestinal retinol dehydrogenases. J Biol Chem. 2006; 281:37828–37835. [PubMed: 17028196]

18. Phelps RA, Chidester S, Dehghanizadeh S, Phelps J, Sandoval IT, Rai K, Broadbent T, Sarkar S, Burt RW, Jones DA. A two-step model for colon adenoma initiation and progression caused by APC loss. Cell. 2009; 137:623–634. [PubMed: 19450512]
19. Zhang Q, Yoshimatsu Y, Hildebrand J, Frisch SM, Goodman RH. Homeodomain interacting protein kinase 2 promotes apoptosis by downregulating the transcriptional corepressor CtBP. Cell. 2003; 115:177–186. [PubMed: 14567915]
20. Wang SY, Iordanov M, Zhang Q. c-Jun NH2-terminal kinase promotes apoptosis by down-regulating the transcriptional co-repressor CtBP. J Biol Chem. 2006; 281:34810–34815. [PubMed: 16984892]
21. Kovi RC, Paliwal S, Pande S, Grossman SR. An ARF/CtBP2 complex regulates BH3-only gene expression and p53-independent apoptosis. Cell Death Differ. 2010; 17:513–521. [PubMed: 19798104]
22. Achouri Y, Noel G, Van Schaftingen E. 2-Keto-4-methylthiobutyrate, an intermediate in the methionine salvage pathway, is a good substrate for CtBP1. Biochem Biophys Res Commun. 2007; 352:903–906. [PubMed: 17157814]
23. Hilbert BJ, Grossman SR, Schiffer CA, Royer WE Jr. Crystal structures of human CtBP in complex with substrate MTOB reveal active site features useful for inhibitor design. FEBS Lett. 2014; 588:1743–1748. [PubMed: 24657618]
24. Friesner RA, Murphy RB, Repasky MP, Frye LL, Greenwood JR, Halgren TA, Sanschagrin PC, Mainz DT. Extra precision glide: docking and scoring incorporating a model of hydrophobic enclosure for protein-ligand complexes. J Med Chem. 2006; 49:6177–6196. [PubMed: 17034125]
25. Booth MP, Conners R, Rumsby G, Brady RL. Structural basis of substrate specificity in human glyoxylate reductase/hydroxypyruvate reductase. J Mol Biol. 2006; 360:178–189. [PubMed: 16756993]
26. Sigurskjold BW. Exact analysis of competition ligand binding by displacement isothermal titration calorimetry. Anal Biochem. 2000; 277:260–266. [PubMed: 10625516]
27. Kumar V, Carlson JE, Ohgi KA, Edwards TA, Rose DW, Escalante CR, Rosenfeld MG, Aggarwal AK. Transcription corepressor CtBP is an NAD(+)-regulated dehydrogenase. Mol Cell. 2002; 10:857–869. [PubMed: 12419229]
28. Alvarez JA, Gelpi JL, Johnsen K, Bernard N, Delcour J, Clarke AR, Holbrook JJ, Cortes A. D-2-hydroxy-4-methylvalerate dehydrogenase from Lactobacillus delbrueckii subsp. bulgaricus. I. Kinetic mechanism and pH dependence of kinetic parameters, coenzyme binding and substrate inhibition. Eur J Biochem. 1997; 244:203–212. [PubMed: 9063465]
29. Dubrow R, Pizer LI. Transient kinetic studies on the allosteric transition of phosphoglycerate dehydrogenase. J Biol Chem. 1977; 252:1527–1538. [PubMed: 320209]
30. Dubrow R, Pizer LI. Transient kinetic and deuterium isotope effect studies on the catalytic mechanism of phosphoglycerate dehydrogenase. J Biol Chem. 1977; 252:1539–1551. [PubMed: 14154]
31. Grant GA, Schuller DJ, Banaszak LJ. A model for the regulation of D-3-phosphoglycerate dehydrogenase, a Vmax-type allosteric enzyme. Protein Sci. 1996; 5:34–41. [PubMed: 8771194]
32. Blevins MA, Kouznetsova J, Krueger AB, King R, Griner LM, Hu X, Southall N, Marugan JJ, Zhang Q, Ferrer M, Zhao R. Small Molecule, NSC95397, Inhibits the CtBP1-Protein Partner Interaction and CtBP1-Mediated Transcriptional Repression. J Biomol Screen. 2014 in press.
33. Birts CN, Nijjar SK, Mardle CA, Hoakwie F, Duriez PJ, Blaydes JP, Tavassoli A. A cyclic peptide inhibitor of C-terminal binding protein dimerization links metabolism with mitotic fidelity in breast cancer cells. Chem. Sci. 2013; 4:3046–3057.
34. Balasubramanian P, Zhao LJ, Chinnadurai G. Nicotinamide adenine dinucleotide stimulates oligomerization, interaction with adenovirus E1A and an intrinsic dehydrogenase activity of CtBP. FEBS Lett. 2003; 537:157–160. [PubMed: 12606049]
35. Mani-Telang P, Sutrias-Grau M, Williams G, Arnosti DN. Role of NAD binding and catalytic residues in the C-terminal binding protein corepressor. FEBS Lett. 2007; 581:5241–5246. [PubMed: 17964573]

36. Fjeld CC, Birdsong WT, Goodman RH. Differential binding of NAD+ and NADH allows the transcriptional corepressor carboxyl-terminal binding protein to serve as a metabolic sensor. Proc Natl Acad Sci U S A. 2003; 100:9202–9207. [PubMed: 12872005]

37. Zhang Q, Wang SY, Nottke AC, Rocheleau JV, Piston DW, Goodman RH. Redox sensor CtBP mediates hypoxia-induced tumor cell migration. Proc Natl Acad Sci U S A. 2006; 103:9029–9033. [PubMed: 16740659]

38. Kim JH, Youn HD. C-terminal binding protein maintains mitochondrial activities. Cell Death Differ. 2009; 16:584–592. [PubMed: 19136938]

39. Emsley P, Lohkamp B, Scott WG, Cowtan K. Features and development of Coot. Acta Crystallogr D Biol Crystallogr. 2010; 66:486–501. [PubMed: 20383002]

40. Adams PD, Afonine PV, Bunkoczi G, Chen VB, Davis IW, Echols N, Headd JJ, Hung LW, Kapral GJ, Grosse-Kunstleve RW, McCoy AJ, Moriarty NW, Oeffner R, Read RJ, Richardson DC, Richardson JS, Terwilliger TC, Zwart PH. PHENIX: a comprehensive Python-based system for macromolecular structure solution. Acta Crystallogr D Biol Crystallogr. 2010; 66:213–221. [PubMed: 20124702]

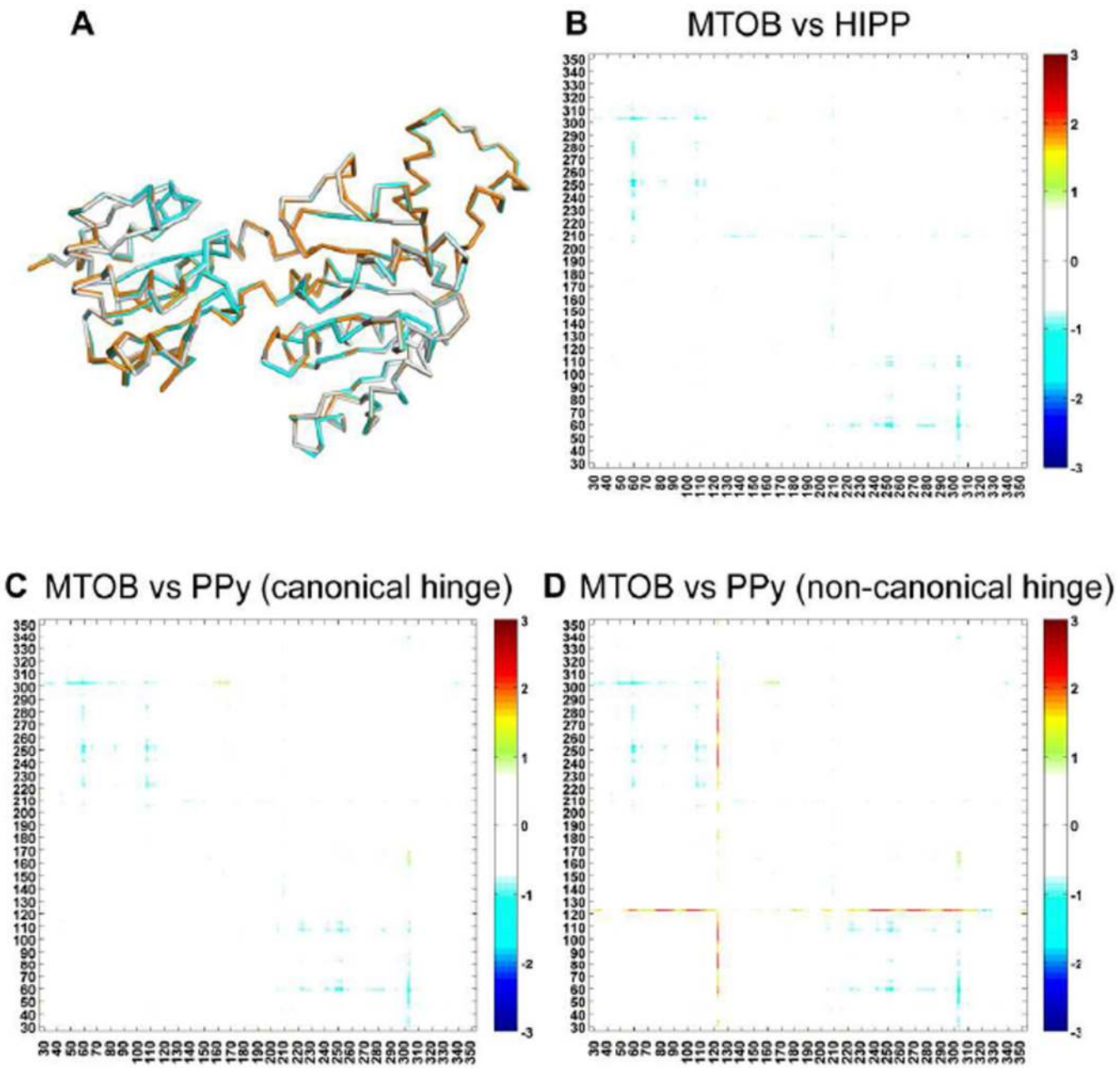

Figure 1.

Ligand binding does not induce major conformational changes. (A) Ribbon diagram of the superposition of the PPy complex (orange) and HIPP complex (cyan) to the MTOB complex (grey). MTOB bound CtBP1 does not differ from apo CtBP1.[23] Therefore, the position of the MTOB complex α-carbons were used for comparison with the HIPP (B) and PPy (C and D) structures. Small differences may be the result of different crystallization conditions relative to the MTOB structure. The phenylpyruvate structure contains a canonical (C) and alternate (D) conformation in the hinge conformation between the substrate binding and coenzyme binding domains. The alternate conformation (D) shows the change in position of

the Cα of residue A123. The shift in position places A123 in the space normally occupied by the active site water network.[23]

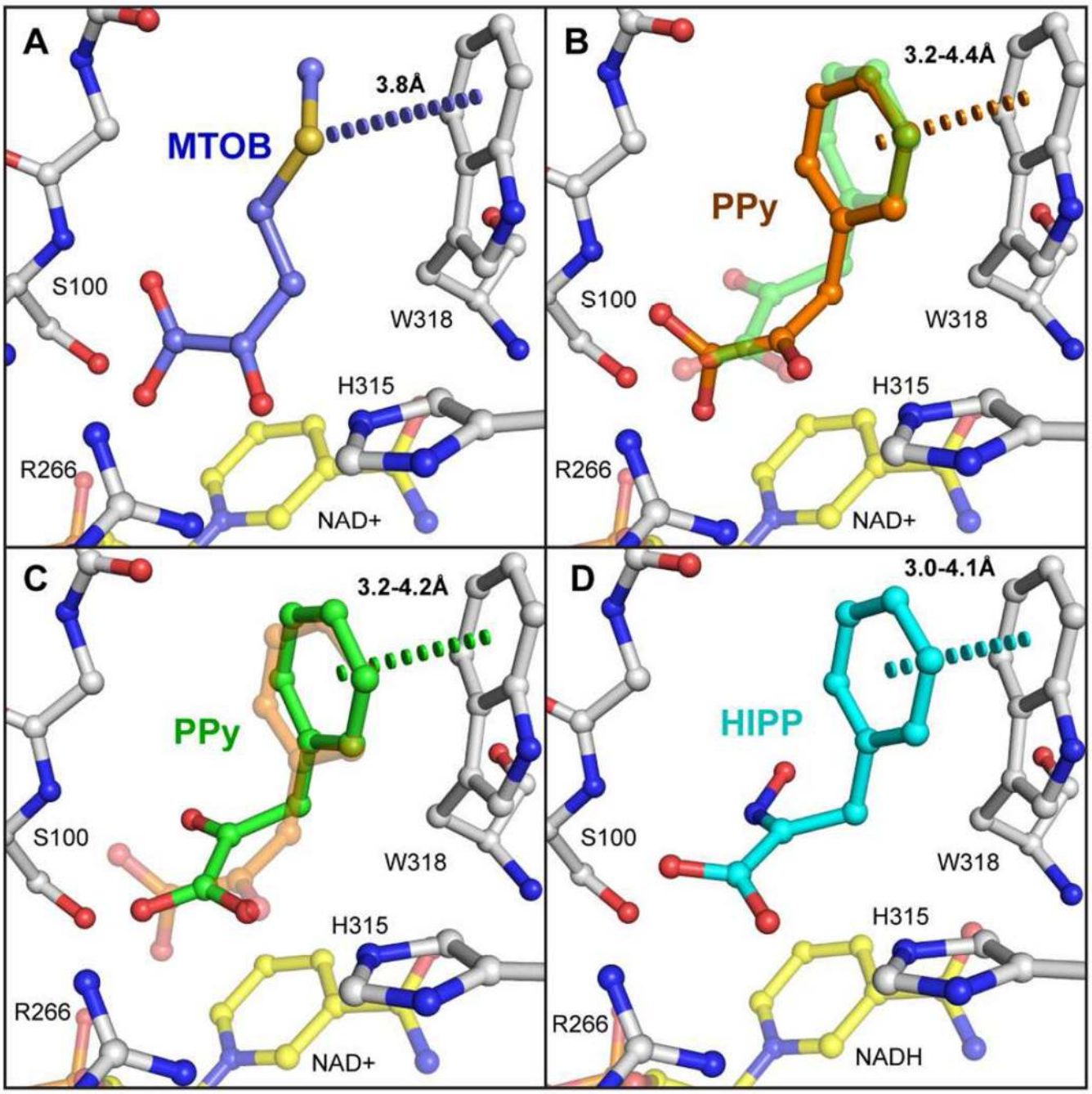

Figure 2.

Two different ligand conformations both strongly interact with W318. (A) MTOB positioned in the CtBP1 active site. A single carboxylate oxygen and the carbonyl oxygen orient towards catalytic residue R266. The sulfur atom rests centered over the indole group of W318, positioned 3.8 Å from the ring at its closest distance (disks). (B) Phenylpyruvate assumes two distinct conformations in the crystal. In the substrate conformation (orange) the PPy positions analogous to MTOB for enzyme catalysis. The atoms of the phenyl group range from 3.2 – 4.4 Å in distance to the nearest atom of the W318 indole group (orange

disks). For comparison, the non-canonical conformation (green) is semi-transparent. (C) The PPy non-canonical conformation (green) repositions the keto acid core of the molecule while maintaining phenyl ring stacking with W318. In this conformation, the phenyl ring positions at a similar distance to W318 of 3.2 – 4.2 Å (green disks). Both carboxylate oxygens orient towards R266, with the carbonyl positioned near S100 instead of catalytic residue H315. (D) HIPP assumes only the non-canonical conformation due to steric hindrance of the hydroxyimino group in the canonical conformation. The hydroxyimino group orients similar to the carbonyl in the noncanonical phenylpyruvate conformation. The phenyl ring stacks 3.0 – 4.1 Å from W318 (cyan disks).

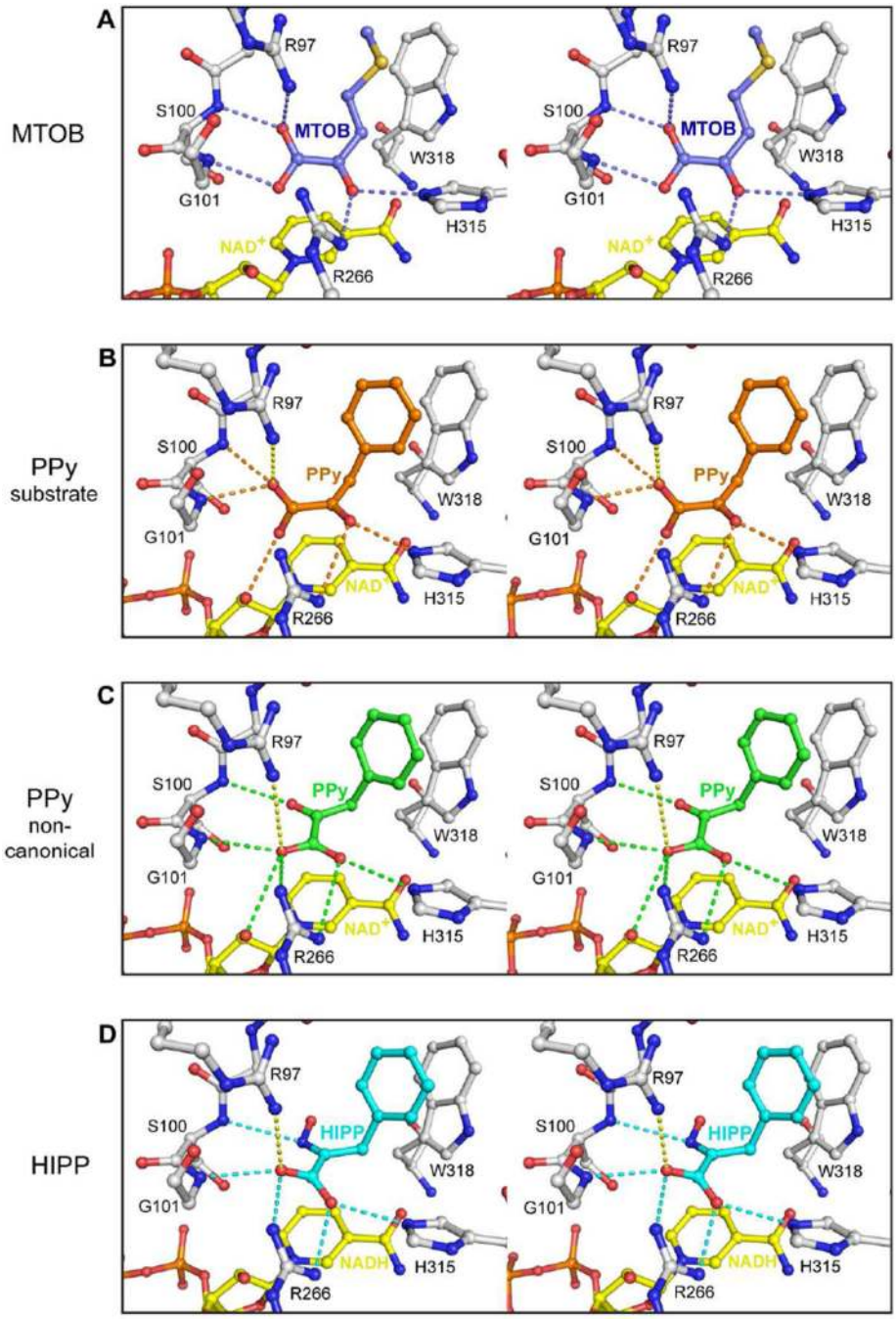

Figure 3.

PPy and HIPP hydrogen bond networks and coulombic interactions shown in stereo. (A) The hydrogen bond network (dashes) of substrate MTOB as previously reported[23] served as a comparison for the new structures. (B) The PPy substrate conformation (orange) possesses a similar hydrogen bond network to MTOB (orange dashes). This conformation has lost the hydrogen bond to R97, although PPy maintains proximity for coulombic interactions (yellow dashes). The substrate PPy has an additional hydrogen bond to the nicotinamide ribose. Conformational changes of NAD^+ obscure this interaction in the MTOB structure.

(C) The noncanonical phenylpyruvate conformation (green) has a distinct hydrogen bond network (green dashes). Orientation of the carboxylate towards R266 maximizes hydrogen bond potential as well as coulombic interactions (yellow dashes) with R97. (D) HIPP (cyan) forms similar hydrogen bonding network (cyan dashes) and coulombic interactions (yellow dashes) to the non-canonical PPy conformation, with the exception of losing the interaction with the nicotinamide ribose.

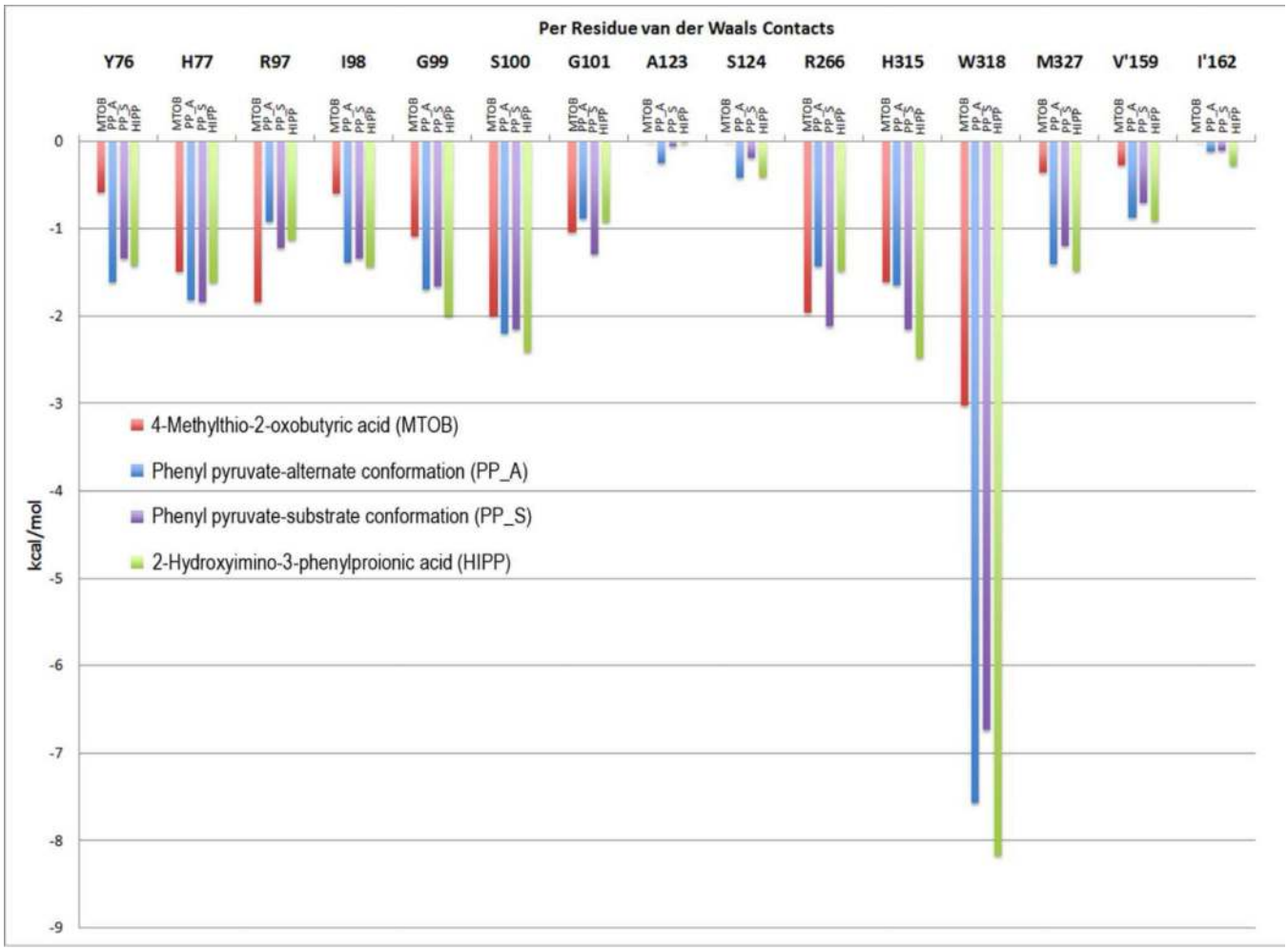

Figure 4.

Calculated van der Waal's contribution to binding energy by residue. PPy and HIPP exhibit more than a 2-fold increase for the calculated van der Waal's contact energy with W318 compared to MTOB. The increased contact with W318 contributes to the increased potency of phenyl pyruvate and HIPP over MTOB. The two alternate PPy conformations have been calculated independently as shown in blue and purple.

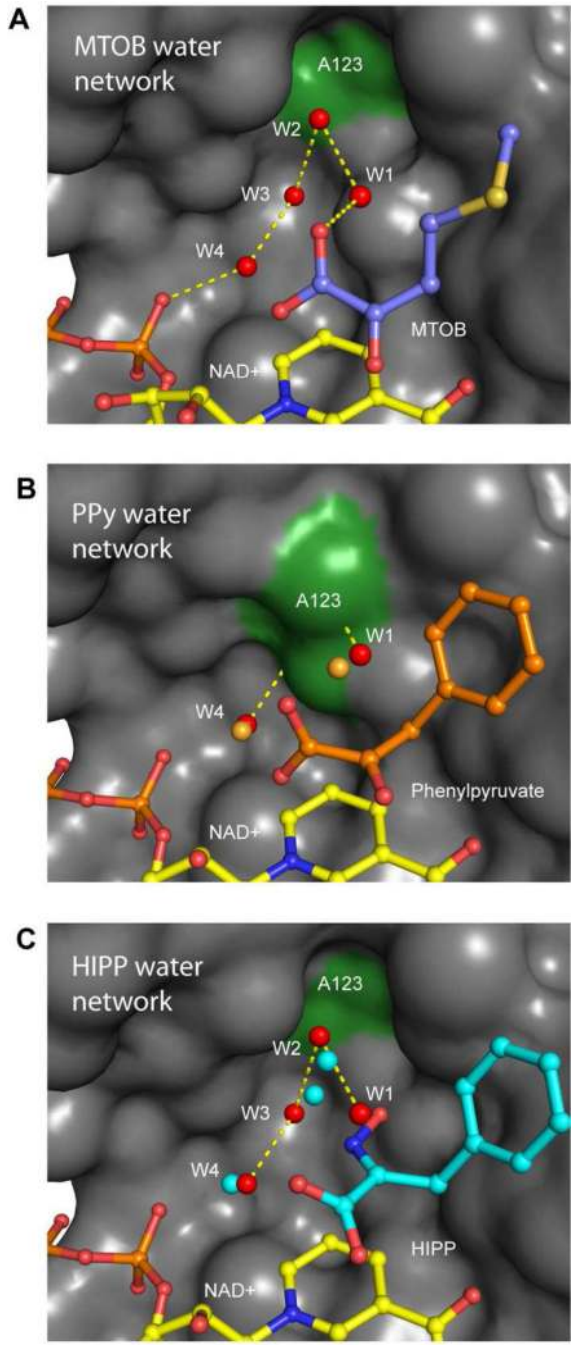

Figure 5.

The effects of ligand binding on the CtBP1 water network. (A) MTOB possesses a water network (red spheres connected by yellow dashes) that connect the substrate to an NAD^+ phosphate via four water molecules (W1–W4). The conformation of hinge residue A123 (dark green) helps create a cavity for the water molecules unique to CtBP. (B) The water network (orange spheres) in the PPy structure is disrupted by the novel conformation of A123. W2 and W3 are completely displaced as the cavity collapses. W1 is present with the substrate conformation of PPy (orange) and when no molecule is bound in the active site

(~60% of the time). (C) The HIPP structure water network is altered by interactions with HIPP. W1 is completely displaced by the HIPP hydroxyl group. W2 has shifted position to interact with HIPP (Figure S4). Due to shifts in both W2 and W3 (now 1.9Å apart), their presence is mutually exclusive. Similar to PPy, HIPP has no effect of W4 position.

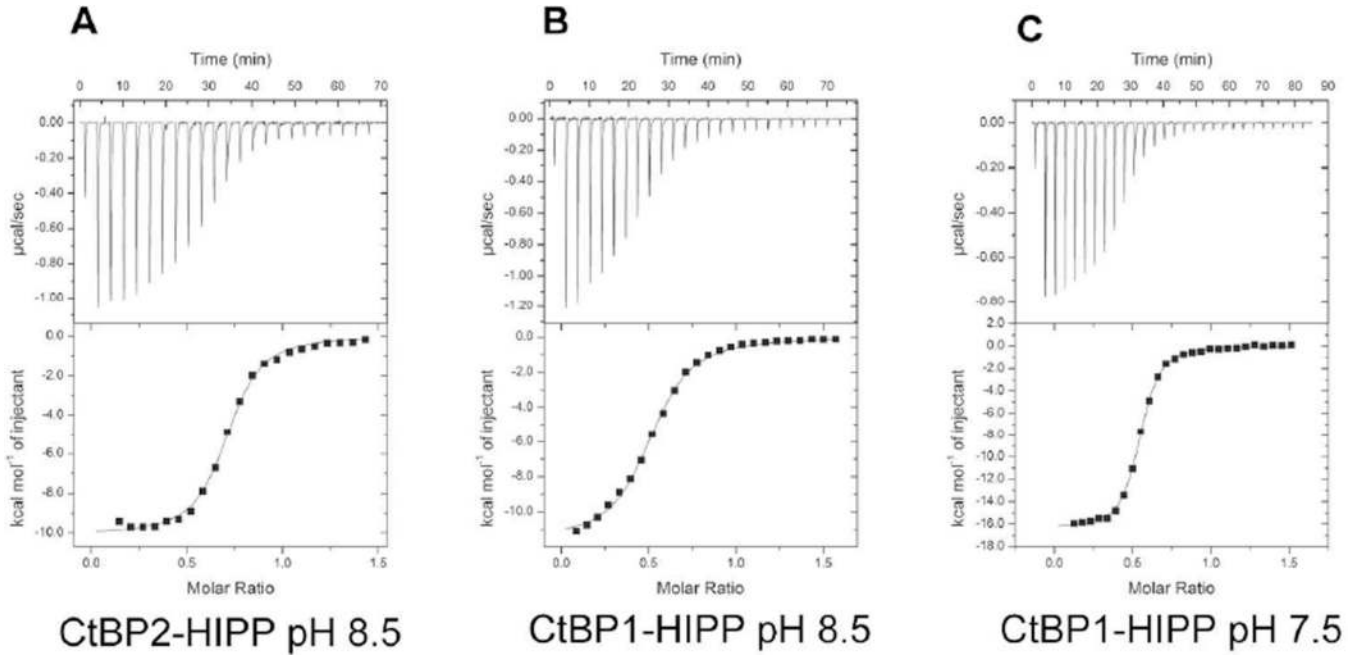

Figure 6.

Example of single ITC experiments utilizing HIPP with (A) CtBP2 at pH 8.5, (B) CtBP1 at pH 8.5, and (C) CtBP1 at pH 7.5. The slope of the line at the midpoint is steeper at pH 7.5, indicating greater HIPP affinity at these conditions. (Full ITC results are provided in Table 1.)

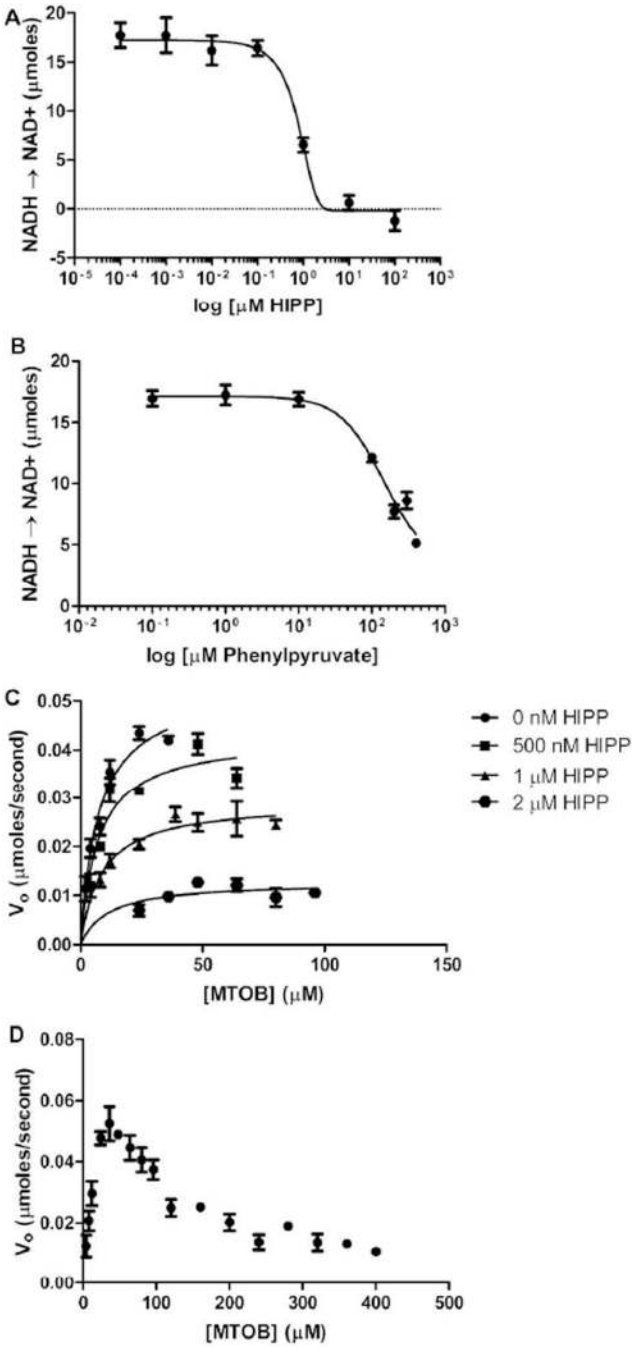

Figure 7.

CtBP inhibition assays. IC_{50} measurements for HIPP (A) and PPy (B) after 15 minutes show that HIPP exhibits an IC_{50} value more than 100 fold lower than PPy. Data represent n=3 and n=2 triplicate experiments, respectively. K_i plots (C) demonstrate that HIPP inhibition results largely from a decrease in V_{max}, which would not be expected for a purely competitive inhibitor. Points represent the average of n=7 reads. MTOB (D) exhibits

substrate inhibition when in excess. n=2 independent triplicate experiments. All error bars represent standard deviation.

Table 1

Thermodynamic parameters for ligand binding to CtBP derived from ITC measurements.[a]

Protein – Ligand	pH	Kd	ΔG (kcal)	ΔH (kcal mol^{-1})	−TΔS (kcal mol^{-1})
CtBP2 - HIPP	8.5	1.30 ± 0.07 μM	−7.9	−10.0 ± 0.08	2.1
CtBP2/NAD$^+$ - HIPP*	8.5	1.44 ± 0.13 μM	−7.8	−10.6 ± 0.24	2.8
CtBP2 - MTOB	8.5	2.96 ± 0.82 mM	−3.4	−3.4 ± 0.34	0.0
CtBP1 - HIPP	8.5	2.77 ± 0.34 μM	−7.5	−11.4 ± 0.31	3.9
CtBP1 – HIPP*	7.5	0.37 ± 0.03 μM	−8.6	−16.7 ± 0.55	8.1
CtBP1 – MTOB**	7.5	1.26 ± 0.36 mM	−3.9	−11.3 ± 0.83	7.4

*Four measurements

**Two Measurements

[a]Values reported represent the average of three measurements, unless otherwise noted.